International Journal of Geo-Information

MDPI

Article

Space–Time Surveillance of COVID-19 Seasonal Clusters: A Case of Sweden

Augustus Aturinde [1,2], Ali Mansourian [1,*]

[1] Department of Physical geography and Ecosystem Science, Lund University, SE-223 62 Lund, Sweden; aaturinde@kyu.ac.ug
[2] Department of Geoinformatics, School of Built Environment, Kyambogo University, Kampala 256, Uganda
* Correspondence: ali.mansourian@nateko.lu.se; Tel.: +46-46-222-1733

Abstract: While COVID-19 is a global pandemic, different countries have experienced different morbidity and mortality patterns. We employ retrospective and prospective space–time permutation analysis on COVID-19 positive records across different municipalities in Sweden from March 2020 to February 2021, using data provided by the Swedish Public Health Agency. To the best of our knowledge, this is the first study analyzing nationwide COVID-19 space–time clustering in Sweden, on a season-to-season basis. Our results show that different municipalities within Sweden experienced varying extents of season-dependent COVID-19 clustering in both the spatial and temporal dimensions. The reasons for the observed differences could be related to the differences in the earlier exposures to the virus, the strictness of the social restrictions, testing capabilities and preparedness. By profiling COVID-19 space–time clusters before the introduction of vaccines, this study contributes to public health efforts aimed at containing the virus by providing plausible evidence in evaluating which epidemiologic interventions in the different regions could have worked and what could have not worked.

Keywords: COVID-19; space–time clusters; retrospective; SaTScan; Sweden

Citation: Aturinde, A.; Mansourian, A. Space–Time Surveillance of COVID-19 Seasonal Clusters: A Case of Sweden. *ISPRS Int. J. Geo-Inf.* **2022**, *11*, 307. https://doi.org/10.3390/ijgi11050307

Academic Editors: Godwin Yeboah and Wolfgang Kainz

Received: 25 March 2022
Accepted: 7 May 2022
Published: 10 May 2022

1. Introduction

Coronavirus disease was first discovered in Wuhan province, China in December 2019 [1] and has since then spread to all parts of the world with it being declared a global pandemic by the World Health Organisation (WHO) in March 2020 when the number of confirmed cases approached 200,000, deaths approached 8000 and cases were reported in 160 countries [2]. COVID-19 is caused by a novel coronavirus whose structure is related to the Severe Acute Respiratory Syndrome (SARS) family of viruses [3] and is characterized by a respiratory illness that sometimes leads to death. Generally, COVID-19 has a death rate estimated to be between 1% and 5% [4]. As of 22 April 2022, the death rate was 1.22% (507,912,123 cases and 6,236,644 deaths), globally [5].

After one year (as of 30 March 2021) into the pandemic, there had been 127 million confirmed cases and 2.7 million deaths, globally [6]. Of those, Sweden had 780,000 confirmed cases and 13,000 deaths [6], representing 0.61% and 0.48% of global cases and death respectively. Given that Sweden's population (10 million) is equivalent to 0.13% of the total world population (7.8 billion), the COVID-19 morbidity and mortality percentages show that the Swedish population was affected more than the average population. While the reasons for this dynamic could be many, it can generally be said that the global north (including Sweden) was more affected by the pandemic than the global south [7].

Several scholars have attributed this disproportionate COVID-19 disease burden in the global north, to among other hypotheses, the fact that this region experiences colder climatic conditions characterized by extended colder winter periods compared to the warmer climatic conditions generally predominant in the global south [8,9]. Cold

temperatures are known to favor the survival of cold viruses as well as reduce immunity in humans by modifying the body's cellular and molecular response to infections in the upper respiratory tract [10]. That said, it is unclear whether these geographically seasonal conditions fully explain the observed disease burden disparity in the two regions. As such, Adedokun, Olarinmoye [11] submitted in their conclusion, that there was a need for more studies to characterize and identify the potential seasonality of COVID-19 cases.

The study of the seasonality of COVID-19 has, since the start of the pandemic, interested the research community [12]. This search is hinged on the premise that if the pandemic responds to or is significantly influenced by the seasons, its manifested spread would show similar patterns. For example, Zoran, Savastru [13] through their study of seasonal factors and COVID-19 waves in Madrid, Spain found that air temperature, relative humidity, air pressure and wind speed had a significant influence on COVID-19 spread with the pandemic having elevated incidence during winter–spring seasons and lower incidences during the summer seasons.

Additionally, through their comprehensive review study on the impacts of temperature, humidity and other meteorological factors (precipitation, solar radiation, wind speed) at a global level (USA, Norway, India, Singapore, China, Brazil, Turkey, Netherlands, and Mexico), Byun, Heo [14] qualified COVID-19 as seasonal evidenced by its inverse relationship with temperature and humidity. They, however, highlighted that local region analyses had drawn ambiguous conclusions, especially on the effect of humidity on COVID-19 transmission, hence advocated for further local scale studies to better understand COVID-19 seasonality—given that now the full seasonal cycle case data are available.

Studies utilizing the full season cycle case data are still few. For Sweden, the Swedish Board of Health and Welfare [15] publishes an overview of the COVID-19 situation but fewer studies have gone in-depth to identify clusters of high disease case burden and the seasons when this burden was prevalent. This study sets out to analyze the season-specific spatiotemporal clustering of COVID-19 cases as officially reported in Sweden. It seeks to do so for a period before the introduction of the nationwide immunization campaigns. The full season cycle before immunization was chosen because we believe immunization altered the original pandemic dynamics from its otherwise 'natural' trends. That said, it is also appreciated that the lockdown and social distancing measures implemented in the country [16] could have influenced the case patterns obtained in this analysis [17].

Moreover, even within the same country (Sweden in this case), not all regions are affected the same way. From an individual-level survival standpoint, Drefahl, Wallace [18] attributed this general spatial disproportionality in the COVID-19 mortality burden across regions in Sweden to the interaction of the virus causing COVID-19 and its social environment. They thus explained that generally being male, having less disposable income, lower education, and being unmarried independently predisposed one to higher risks of death from COVID-19. At a county-level, Gémes, Talbäck [19] used prognostic analysis to underscore the relative interplay between having existing underlying health conditions of being above 70 years, having Cardiovascular disease, cancer, chronic obstructive pneumatic/pulmonary disease (COPD), severe asthma or diabetes, and their contribution to severe COVID-19. They particularly stressed the need to spatially visualize nationwide patterns to aid targeted epidemiologic planning and intervention.

For effective targeted intervention, the relative local disease burden needs to be evaluated before apportioning proportionate epidemiologic responses. Numerous spatial and/or temporal methods have previously been used to evaluate such relativity in local disease burden including but not limited to the use of Geographical Analytical Machine (GAM) to investigate leukemia clusters in the north of England by Openshaw, Charlton [20]. The use of other spatial methods was extensively discussed by Pullan, Sturrock [21] as well as the application of space–time scan statistics [22].

The use of space–time scan statistics is specifically important for timely surveillance of emerging clusters as has been applied in clustering of shigellosis [23,24], thyroid cancer

[25], measles [26,27], and more importantly COVID-19, as was used by Hohl, Delmelle [28] and Desjardins, Hohl [29] in the USA, Gomes, Andrade [30] in Brazil, Masrur, Yu [31] in Bangladesh, to mention but a few. Being an ongoing pandemic, detailing the areas where the disease has been more prevalent or where it is currently more prevalent is informative to epidemiologic preparation, resource appropriation and deployment of medical personnel.

To this end, our current study proposes to cast the observed spatial clusters in the light of the seasons existing in Sweden. This way, different socio-economic activities within the different seasons and especially those that promote social gathering or social isolation can be used to plausibly explain the patterns of COVID-19 cases observed. As a result, the study is aware of the modifying influence of the numerous restrictions that were implemented during this time. Nonetheless, we are convinced that seasonality provides clues on how the pandemic was managed. Moreover, the study period was chosen in such a way that it avoids the influence of adult COVID-19 immunization. Therefore, it analyzed the reported cases before the compulsory immunization drives in Sweden.

This study contributes to ongoing COVID-19 surveillance efforts in Sweden by profiling the progression of COVID-19, on a seasonal basis. It also prospectively evaluates the current space–time clusters in the country. This profiling, especially before the introduction of mass vaccination, is informative to the healthcare providers and planners as it provides evidence-based mechanisms to evaluate the different epidemiologic interventions adopted by different regions and how COVID-19 cases responded to such local-level interventions.

The primary aim of this study, therefore, is to evaluate the retrospective and prospective space–time clusters of the COVID-19 epidemic through the four seasons using weekly COVID-19 records at the municipality level in Sweden, provided by the Swedish Public Health Agency (Folkhälsomyndigheten) from March 2020 to February 2021. The rest of the manuscript is organized as follows: Section two handles the data and the applied methods, the third section outlines the results, the fourth section discusses the results and finally, the fifth section provides the conclusions.

2. Materials and Methods

2.1. Data

2.1.1. COVID-19 Data

The COVID-19 records were provided by the Swedish Public Health Agency—Folkhälsomyndigheten [32]. The COVID-19 database is updated daily (for regions). For finer spatial scales (municipality), however, the records are aggregated and provided as weekly updates, in a single downloadable excel file.

The period of analysis was the four seasons of 2020: spring, summer, fall and winter (2020/2021). The starting period (spring, 2020) of the analysis is coincident with the period when COVID-19 cases in Sweden became noticeable (>100 cases). It is also about the same time when it was declared a global pandemic by the World Health Organization [14]. This was the rationale behind starting with week 11, 2020, in the analysis. Sweden and the summary of the COVID-19 case profile for the four seasons are shown in Figure 1.

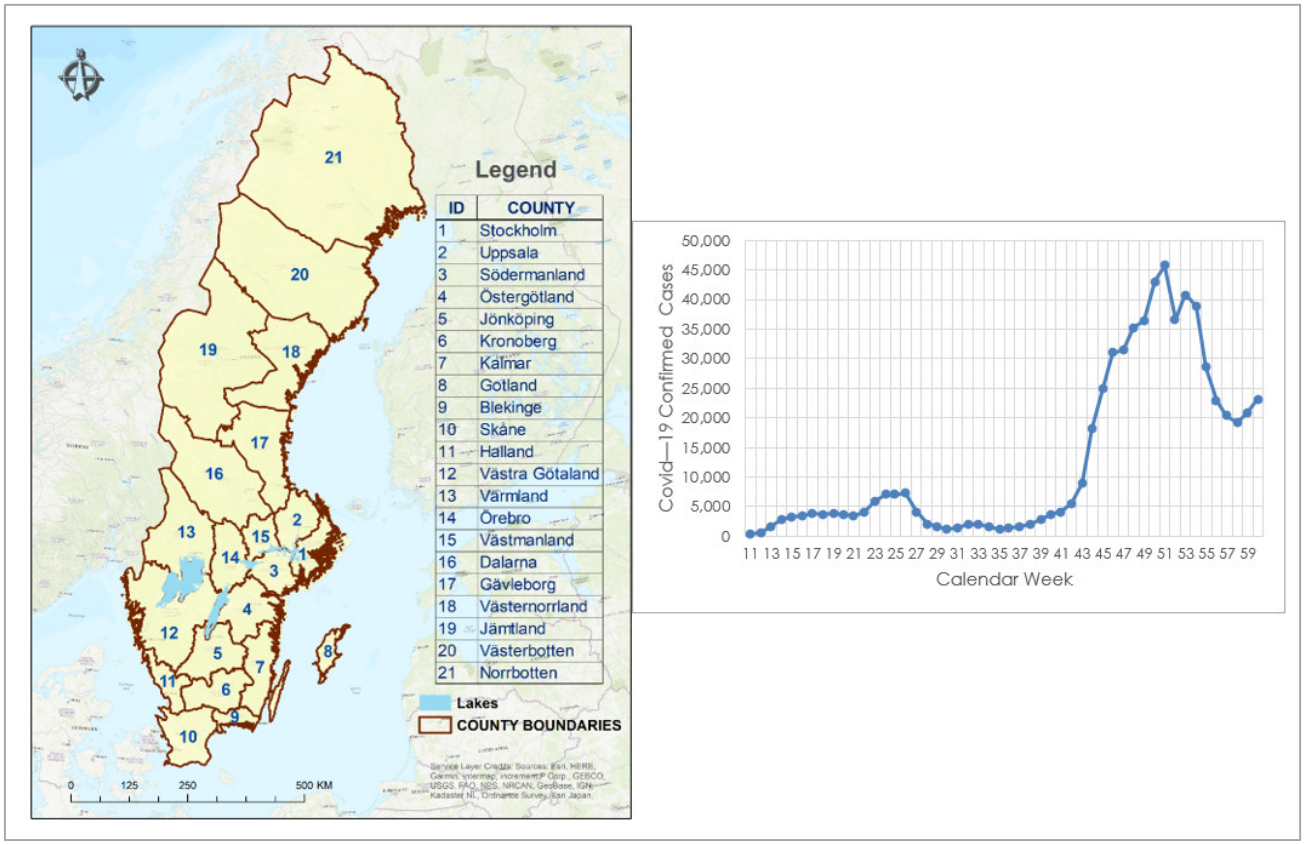

Figure 1. Sweden and its COVID-19 case profile through the seasons (2020).

2.1.2. Municipality Boundaries

The Demographic Statistics Areas (DeSO) digital boundaries data were obtained from Statistics Sweden's Geodata portal [33]. The advantage of using DeSO boundaries is that in addition to being consistent over time (will not change over time), they follow municipality boundaries and aggregate to the municipality level. This ability to aggregate into the municipality was used to collapse the DeSO units into their containing municipalities. This was necessary for interoperability as the COVID-19 weekly data were recorded at the municipality level. The DeSO dataset was provided as a Geopackage (zip file), and the manipulation was completed in ESRI's ArcMap 10.5.

2.2. Methods

Retrospective and Prospective Space–Time Permutation

The space–time permutation scan statistics evaluate existing or active space–time clusters, by utilizing numerous overlapping cylinders to define the scanning window. In this setup, each window has the potential of being an outbreak (cluster), with the base of the cylinder defining the geographical area of the potential cluster [25].

Typically, the window iterates over a finite number of spatial points (municipalities), gradually increasing the circle radius from zero to the predefined maximum value, set by the user. The height of the cylinder represents the temporal dimension (weeks in our case), with the last week always included together with a variable number of preceding weeks until the maximum predefined value (by the user) if the statistic is used in the prospective sense, as used in this study. The space–time permutation deviates from the Poisson and other scan statistics probability models in that it does not require the population-at-risk. This is consistent with COVID-19 reporting that has consistently been reported with the number of cases only (morbidity and mortality) [28].

Suppose we have the weekly case counts for a given municipality, n_{zd} is the number of cases in municipality z during week d. The total number of cases (N) is given in Equation (1).

$$N = \sum_{z} \sum_{d} n_{zd} \tag{1}$$

The expected number of cases for each municipality and week μ_{zd} conditioning on the observed marginals is calculated by Equation (2).

$$\mu_{zd} = \frac{1}{N}\left(\sum_{z} n_{zd}\right)\left(\sum_{d} n_{zd}\right) \tag{2}$$

The expected number of cases μ_B in a particular cylinder, B is the summation of expectations over all the municipality weeks within the cylinder B given by Equation (3).

$$\mu_B = \sum_{(z,d)\in B} \mu_{zd} \tag{3}$$

Based on this approximation, the Poisson generalized likelihood ratio (GLR) is used to indicate whether a given cylinder B is an outbreak (cluster) by comparing the observed and the expected number of cases, within and outside the cylinder, according to Equation (4).

$$GLR = \left(\frac{n_B}{\mu_B}\right)^{n_B} \left(\frac{N-n_B}{N-\mu_B}\right)^{N-n_B} \tag{4}$$

Of the many cylinders evaluated, the one with the maximum GLR constitutes the space–time cluster of cases least likely to have occurred by chance and is considered a candidate for a true outbreak.

Given a large number of spatial locations, sizes and time lengths, the obtained results need to be adjusted for multiple testing problems. In the absence of population-at-risk, this is achieved by creating a large number of random permutations in both spatial and temporal attributes of each case in the dataset, ensuring that the marginals remain unchanged. Then the most likely cluster is computed for this simulated dataset as was done for the real data. The statistical significance was evaluated using Monte Carlo hypothesis testing. Under the prospective settings, the null occurrence rate is reported too—the expected time between observing an outbreak signal with equal or higher GLR, under the null hypothesis. It is calculated as every $1/p$ temporal units [29].

Having tested for sensitivity, this analysis retained the default upper bounds for the spatial window (50% of the population at risk), while the temporal maximum cluster size was set to 50% of the study period. The minimum temporal cluster size was set to 3 weeks, with the minimum number of cases in a cluster set to 10.

3. Results

3.1. COVID-19 Reported Cases Profile

The summary statistics for the reported cases from the declaration of the disease as a pandemic (week 11) to the last month (week 60) just before the implementation of nationwide immunization were as follows. Nationally, there were 627,338 confirmed cases during the study period. The national weekly average case count was 12,547 while the median weekly case count was 4174 cases. Graphically, the trends were summarized as shown in Figure 2.

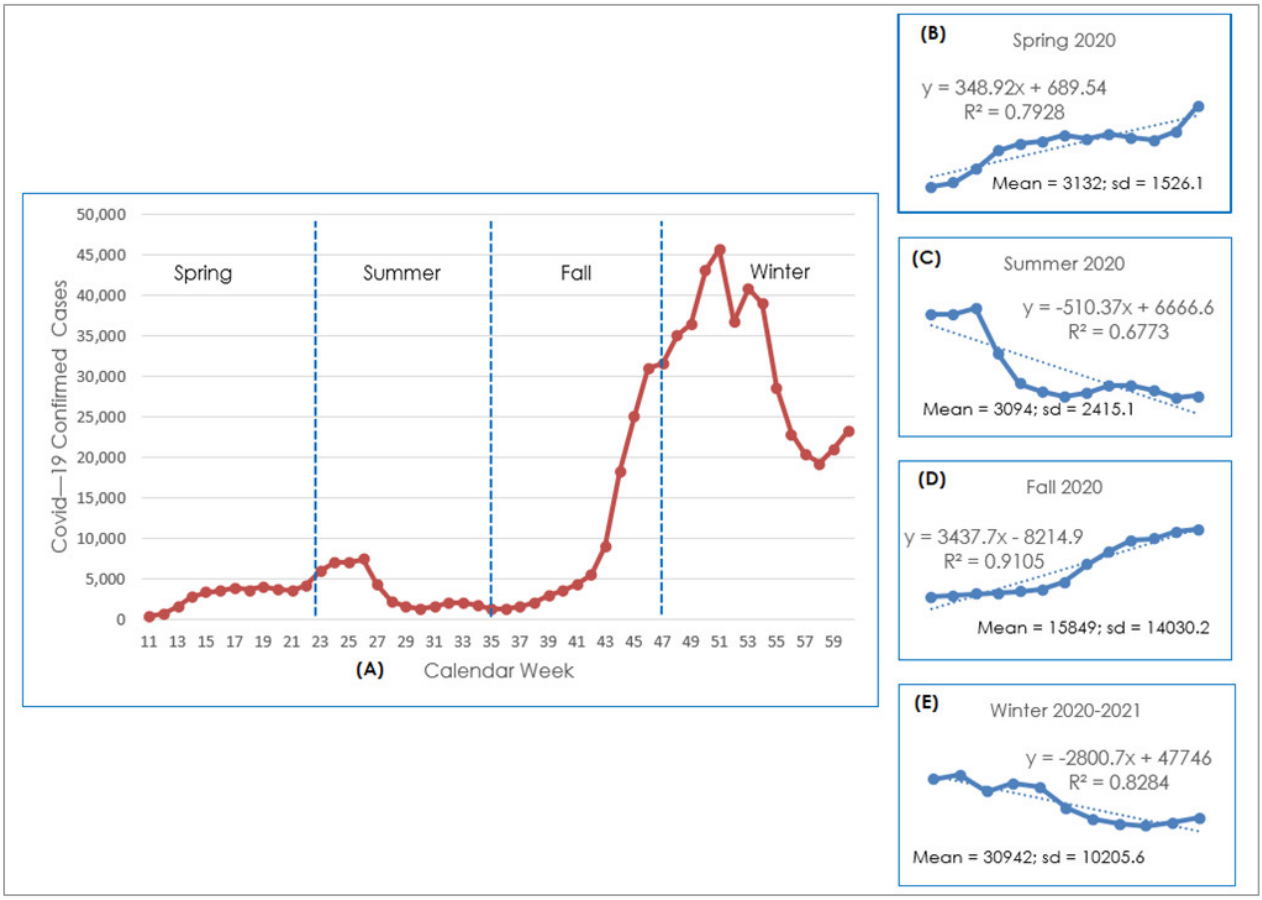

Figure 2. COVID-19 weekly reported cases within the four seasons. (**A**) shows the general trends for all the seasons; (**B**) shows the trend in Spring; (**C**) shows the trend in Summer; (**D**) shows the trend in Fall; and (**E**)shows the trend in Winter.

Figure 2A shows that generally, there was a rise in the cumulated weekly COVID-19 reported cases from spring 2020 to summer 2020 with a slight decline within the summer season. The fall season of 2020 was characterized by an almost exponential increase in the number of reported cases. The peak was in the first weeks of the winter season (week 52). This was followed by a sharp fall in the number of reported cases as the winter season progressed before another increase in weeks 57–60 of the winter 2020–2021.

The individual subsequent seasons are characterized by almost opposing patterns as shown by the seasonal graphs on the right of Figure 2B–E. The spring season (Figure 2B) for example shows a gradual increase in the number of reported cases, while the summer season (Figure 2C) depicts a sharp fall in the cases before the numbers are sustained at almost the lowest level. The fall season (Figure 2D) on the other hand shows a rise in the cases again, this time a sharper rise. The winter season (Figure 2E) shows a decline in the cases before another rise in the cases towards the end. In terms of absolute numbers, the mean weekly cases recorded started at 3132 in spring, to 3094 in summer, to 15,849 in fall and 30,942 cases in winter.

While these general trends at the national level are informative, especially given their breakdowns into the different seasons, Figure 2 does not show the areas where the case burden was more, hence not pinpointing the areas of priority. This was resolved in this study through space–time permutation analysis of the reported cases for the four seasons.

The COVID-19 clusters that existed within each season and those that persisted to the end of each season were analyzed using the two variants of space–time permutation analysis (retrospective and prospective). The retrospective analysis evaluates clusters that existed within the period of analysis. As the nature of the retrospective analysis is backwards-looking, and, as shown from our tests, it is not (very) sensitive to the clusters that

were emerging at the end of each season. To evaluate for emerging clusters and clusters that were still persistent as the seasons were ending, the prospective variant of space–time permutation analysis was applied. The two resulting sets of clusters were then spatially overlaid for visualization, interpretation and discussion. For visualization, the retrospective clusters are labelled in this paper with their weeks of occurrence while the prospective clusters are labelled with numbers (blue) as their other details are given in the tables. To this end, Figure 3 is used to visualize the spatiotemporal clusters within the four seasons of analysis (spring 2020, summer 2020, fall 2020, and winter 2020/21).

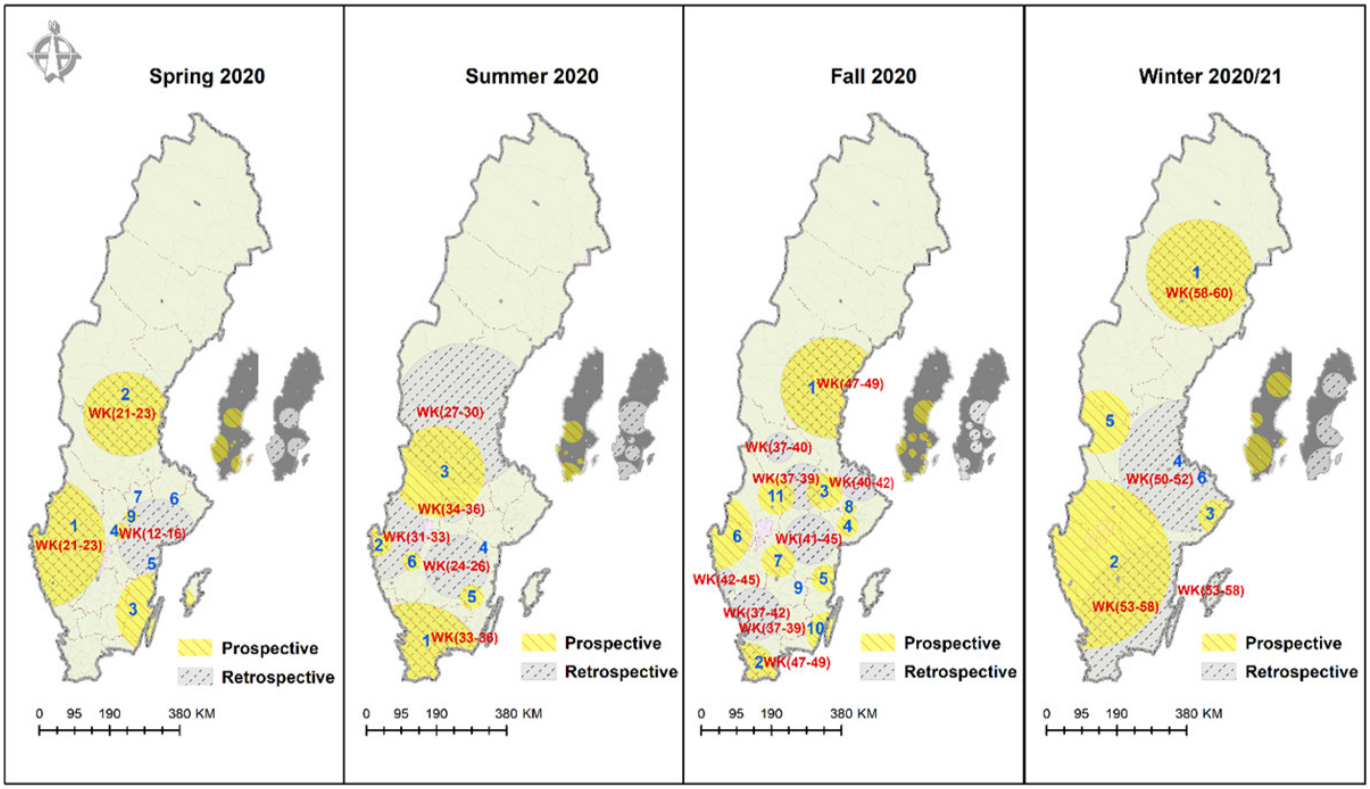

Figure 3. Retrospective and prospective space–time clusters through the seasons.

Figure 3 shows the clusters from the retrospective and prospective space–time analysis. From a general perspective, Figure 3 brings to the fore three aspects that are worth further probing: (1) There was a general movement of the COVID-19 case clusters towards the north as seasons progressed (general 'northification' of the clusters); (2) Larger clusters were observed in summer and winter when compared with those obtained in the spring and fall seasons. This aspect becomes clearer with the calculation of average cluster diameter in Table 1; (3) The number of clusters increases during the spring and fall seasons. However, these clusters, though numerous, are smaller than those in the summer and winter seasons.

In terms of numbers, the spring season had 3 retrospective clusters and 9 prospective clusters. The summer season had 5 retrospective clusters and 6 prospective clusters. The fall season had the highest number of clusters with 9 retrospective clusters and 11 prospective clusters. Finally, the winter season had 4 retrospective clusters and 6 prospective clusters. Going by the number of clusters, it can be inferred that the retrospective analysis is less sensitive than the prospective analysis. This was especially so when the clusters appeared towards the end of the season. For this reason, the prospective clusters are subsequently given more attention.

The precise details of the prospective clusters are given in Table 1. These characteristics include the cluster number, the duration, significance measure (p and t-Statistic), the

observed cases, the expected cases, the ratio of observed to expected (O/E), the number of municipalities involved and the cluster diameter in kilometers.

Table 1. Characteristics of the prospective spatiotemporal clusters (weeks 11–60).

Cluster	Duration	*p*	t-Statistic	Observed (O)	Expected (E)	O/E	# Muni	Diameter (KM)	
1	weeks 21–23	<0.001	323.65	4170	2785.46	1.50	57	181.65	SPRING 2020
2	weeks 21–23	<0.001	107.15	713	391.60	1.82	12	113.67	
3	weeks 21–23	<0.001	43.57	342	197.46	1.73	14	109.86	
4	weeks 19–23	<0.001	13.78	192	128.23	1.50	3	23.68	
5	weeks 20–23	<0.001	10.57	45	20.77	2.17	1	0.00	
6	weeks 21–23	<0.001	8.17	43	21.64	1.99	1	0.00	
7	weeks 21–23	<0.001	7.79	18	5.99	3.00	1	0.00	
8	weeks 19–23	0.004	6.74	39	20.33	1.92	1	0.00	
9	weeks 20–23	0.008	6.23	52	30.52	1.70	2	18.31	
1	weeks 33–36	<0.001	395.94	1616	740.03	2.18	45	190.81	SUMMER 2020
2	weeks 31–36	<0.001	76.63	235	92.65	2.54	7	41.29	
3	weeks 34–36	<0.001	43.34	288	157.72	1.83	29	123.54	
4	weeks 33–36	<0.001	19.85	110	56.47	1.95	1	0.00	
5	weeks 34–36	<0.001	12.58	26	8.03	3.24	3	32.81	
6	weeks 31–36	0.007	9.19	73	42.24	1.73	3	25.90	
1	weeks 47–49	<0.001	308.36	4978	3438.12	1.45	13	135.63	FALL 2020
2	weeks 47–49	<0.001	168.98	14,072	12,063.93	1.17	22	77.46	
3	weeks 47–49	<0.001	51.7	4414	3778.33	1.17	10	49.24	
4	weeks 47–49	<0.001	39.97	6266	5593.95	1.12	8	30.01	
5	weeks 47–49	<0.001	34.92	567	390.74	1.45	2	37.89	
6	weeks 47–49	<0.001	30.18	2334	1980.22	1.18	17	104.62	
7	weeks 45–49	<0.001	14.32	2860	2585.05	1.11	12	45.29	
8	weeks 46–49	<0.001	12.29	4637	4310.98	1.08	6	19.11	
9	weeks 47–49	<0.001	11.11	289	216.13	1.34	1	0	
10	weeks 47–49	<0.001	9.07	1146	1008.12	1.14	6	58.28	
11	weeks 47–49	<0.001	5.95	463	392.74	1.18	8	49.86	
1	weeks 58–60	<0.001	894.56	2650	1025.94	2.58	14	143.97	WINTER 2020/21
2	weeks 56–60	<0.001	444.40	47,387	41,581.47	1.14	128	228.23	
3	weeks 58–60	<0.001	36.40	9011	8234.66	1.09	12	45.92	
4	weeks 58–60	<0.001	30.27	1048	816.17	1.28	1	0	
5	weeks 57–60	<0.001	29.71	289	176.99	1.63	3	85.52	
6	weeks 58–60	<0.001	15.05	170	108.14	1.57	1	0	

3.2. Municipality-Level Results—Spring 2020 (Week 11—Week 23)

Table 1 shows the characteristics of the prospective significant clusters for the whole study period. It shows that most clusters for the spring season were from week 21 to week 23 (clusters 1–3, 6, 7), including the biggest cluster in the southwestern parts of Sweden. It can also be observed that apart from the first 4 clusters (>100 cases), the observed cases were still few. Additionally, 4 of the 9 clusters were single-site clusters (cluster diameter of 0.00). The mean and standard deviation of the observed cases were 623.8 and 1349, respectively.

The location of these space–time clusters that persisted until the end of the spring season can be seen in Figure 3 (leftmost panel). It shows that 3 major clusters were persistent until the end of the spring season, much as there were 9 significant clusters in total. These were mainly in the southwest (Kalmar County), south-east (Västra Götaland and

Värmland counties) and another cluster around Gävleborg county. It also shows that Stockholm and its surrounding areas were still free of any clusters. The same is true for the Skåne region at the south-most end of Sweden.

The spring retrospective clusters in Figure 3 show an early cluster around Stockholm and the surrounding counties of Östergötland, Södermanland and Västmanland. These specific clusters occurred very early into the pandemic around the 12th to the 16th week of 2020. The other clusters identified were coinciding with the clusters from the prospective analysis in both the spatial and temporal dimensions—Västra Götaland and Gävleborg in weeks 21–23.

3.3. Municipality-Level Results—Summer 2020 (Week 24—Week 36)

Table 1 also provides the statistical characteristics of the space–time clusters that persisted to the end of the summer season of 2020. There were 6 significant space–time clusters, with the largest being about 190 km in diameter while the smallest was a single location cluster. The range of observed cases was 1616–1626 while the mean and standard deviation were 391.3 and 608.1, respectively.

From the standpoint of the location of the clusters, the summer prospective clusters were distributed around Sweden with most of them to the south of the country. Figure 3 (second left panel) shows the location of these clusters. The biggest cluster consisted of Skåne, Blekinge, Kronoberg and Halland counties. The second-largest cluster was centred around Dalarna County. The other 3 clusters were in Kalmar and Västra Götaland counties.

The summer retrospective clusters in Figure 3 were also mainly in the southern parts of Sweden and existed between the weeks 24–26 around Östergötland county, weeks 27–30 around Gävleborg and Dalarna counties and weeks 33–36 around Skåne and its northward bounding counties of Kronoberg Blekinge and Halland.

3.4. Municipality-Level Results—Fall 2020 (Week 37—Week 49)

Additionally, Table 1 outlines the fall season prospective cluster statistics. It can be observed that the number of significant clusters was the highest during this season. There were 11 clusters altogether with the largest spanning about 135 km and the smallest being 30 km with one single location cluster. The range of the observed cases was 14,072–289—the mean was 3820.5 while the standard deviation was 3975.5.

The fall season was characterized by an increased number of clusters as given in Figure 3 (second right panel). There were 11 significant clusters, even when only nine seem visibly distinct. The biggest cluster was located north of Stockholm around Västernorrland and Gävleborg counties; the second largest was located in the southwest around Västra Götaland and Värmland regions; the third largest was located around the Skåne region. Other relatively smaller clusters were around the Kalmar region, Stockholm and Uppsala regions and the areas westerly of Stockholm towards Västra Götaland.

For the fall season retrospective clusters in Figure 3, their numbers were the highest with most of them minimally intersecting the prospective clusters if at all. These were mainly in Uppsala, Dalarna, Östergötland, and Halland. The retrospective clusters around Skåne and Västernorrland County overlapped with the prospective clusters for weeks 47–49.

3.5. Municipality-Level Results—Winter 2020/21 (Week 50—Week 60)

The final segment of Table 1 provides the statistics for the space–time clusters that persisted during the winter season of 2020/21. It shows that there were 6 significant clusters with the biggest spanning some 228 kilometers and 2 of the clusters being single location clusters. The observed cases for the different clusters ranged from 47,387 for cluster 2 to 170 for cluster 6. The range, the mean and standard deviation of the observed cases were 47,387–170, 10,092.5 and 18,567.8, respectively.

The spatial distribution for the prospective clusters in the winter season is depicted in Figure 3 (rightmost panel). It shows that the largest cluster covers most areas around the southwestern parts of the country, excluding the Skåne and Blekinge counties. The second largest is located to the north of the country and includes municipalities within the counties of Västerbotten and Norrbotten. The third-largest is located to the west and includes municipalities within Dalarna County. The last non-single-location cluster includes municipalities within Stockholm County.

The summer retrospective clusters in Figure 3 show fewer but extensive easterly clusters in the mid-northern parts (Västerbotten), the middle counties (Stockholm, Dalarna, Uppsala, and Gävleborg) and the southern counties (Skåne, Blekinge, Kalmar, Jönköping, Östergötland, and Gotland) of Sweden. Only the mid-northern cluster coincides with the prospective cluster in space and time (weeks 58–60).

4. Discussion

This study set out to analyze the space–time clusters of COVID-19 morbidity in Sweden, one year since it was declared a global pandemic. We utilized both the retrospective and prospective space–time permutation scan statistics to detect clusters that were present within the seasons and those that were persistent until the end of the four seasons (spring, summer, fall and winter), stretching from 2020 week 11 to week 60 (week 7 of 2021). The prospective scanning statistic is valuable to epidemiologic surveillance as it helps to identify clusters that are emerging or active during a specific period, hence helping health departments in monitoring and potentially intervening promptly [29].

Moreover, when used with the permutation procedure as applied in this study, the scan statistic is robust with both normal and non-normal data [15,33]. The advantage of using the statistic, in both the retrospective and prospective settings, lies in our observation that when used in just one of the settings alone, some space–time clusters are missed. For example, when used in a retrospective sense, we observed that the statistic (always) missed some of the space–time clusters that were identifiable with the prospective setting, and vice versa. By the nature of the prospective analysis, the set-up allows for the inclusion of the new cases as they come and the analysis is re-run [24]. This way, it can help in tracking the nature of the clusters, whether they are expanding, shrinking or stable over time. Whereas this specific aspect of updating and re-running is not pursued in this exploratory paper, it is an aspect that can be taken advantage of.

Equally, the clusters that existed within the seasons, but faded before the seasons ended, were analyzed using the retrospective version of the space–time permutation analysis. The start and end weeks for both analyses were the same (as with prospective), with the benefit of obtaining clusters that were coincident in both space and time dimensions—thereby confirming the specificity of each of the two space–time analysis versions. To this end, it should be stressed that for all the clusters that overlapped 100% in the spatial aspect, they also coincided temporally.

The spring season of 2020 marked the spread of COVID-19 globally and its declaration as a global pandemic [6]. It is also the time when COVID-19 in Sweden became noticeable (cases > 100) [16]. That said, unlike other European and Scandinavian countries (Denmark, Norway, Finland), Sweden imposed fewer legal restrictions in the form of total lockdowns and instead relied on the population to comply with government advice and recommendations on COVID-19 containment and prevention [34]. Possibly resultantly, there was excess mortality during the first COVID-19 wave when compared with other Scandinavian neighbors [35].

From our retrospective results, the early space–time clusters occurred from week 12 to week 16 of 2020 and were in Stockholm and its surrounding counties of Östergötland, Södermanland and Västmanland. Interestingly, the prospective analysis had missed out on this early cluster around Stockholm, inconsistent with COVID-19 reports in early spring 2020 [36]. Later, in weeks 21–23, the space–time clusters were around Kalmar, Västra Götaland, Värmland and Gävleborg counties. The specific drivers for these early

clusters could be linked to early exposures, possibly due to travelers that became sources for community transmission of COVID-19 in the different clustered areas and areas in their surroundings [37]. It could also be true that other areas also had some cases (and possibly clusters in early spring) but were left undetected due to a lack of readiness to test and detect COVID-19 as it was still a new epidemic whose confirmatory tests were still developing at the time. From the mean and standard deviation of the observed cases, this period had the least number of cases.

Generally, there was a reduction in the number of observed COVID-19 cases for the summer season of 2020. This downshift, while it could be linked to the different county health authorities adjusting to COVID-19 cases by imposing stricter health guidelines in terms of social distancing [17], it could also be linked to the general decrease of common flu prevalence whenever ambient temperatures increase [12] as observed in a related study in Belgium [38]. This could also be true for COVID-19 observed patterns. The space–time clusters that persisted until the end of summer were generally in areas around Skåne, Dalarna, and Västra Götaland. Some of the general driving factors could be linked to the increased movement of people and general outdoor activity during this season. This thinking of increased outdoor activity and interaction is consistent with the results obtained by Venter, Barton [39] in Norway.

The fall season saw a rise in the number of cases and a general increase in the number of space–time clusters. The clusters were located in all major cities in Sweden (Stockholm, Gothenburg, Malmö, etc.). Additionally, the mean number of observed cases was the highest (3820). This could be linked to the after-effects of the free movement and the increased outdoor activity during the summer season that possibly resulted in increased exposure of the general population. It could also be a result of the outburst of untreated cases within communities—mainly because COVID-19 was initially concentrated in the socially disadvantaged groups of the poor [18] and immigrants [36]. Finally, it is also possible that the testing mechanism of the numerous cities had improved by this time, hence testing more and confirming more cases. This observation is consistent with the increased tightness of the health guidelines in most parts of the country for most regions, during this period [16].

The winter season was characterized by a disproportionate burden of observed cases in the southwestern parts of Sweden. While it can be said that generally flu and colds tend to increase during the winter seasons [14], the driving factors for this observed disproportionate pattern in the south are not clear but could be related to fairly more relaxed social regulations that were prevalent in these regions compared to other regions. The same could be said for other clusters around the capital Stockholm, Dalarna, Västerbotten and Norrbotten counties. The alternating rise and fall of the confirmed cases through the seasons was consistent with the results by Huang [40] even when his study was a global one. He observed intensifying and persistent cold spots in some parts of Sweden, as well as a belt of new hotspots and oscillating hotspots especially in the south and southwestern parts of Sweden, for his period of analysis (22 January 2020 to 22 January 2021).

5. Conclusions

The COVID-19 pandemic has been a global challenge and has brought most of the world to a standstill. We analyzed, and took stock of space–time clusters of the pandemic within Sweden for the past year, considering the different seasons. From our results, it was evident that the clusters were not static in space and time. The clusters seemed to respond to changes in seasons while acknowledging the contribution of socio-economic factors. In all, this analysis provides a profile of COVID-19 spatiotemporal clustering in Sweden before the introduction of mass vaccination and provides pointers towards a possible evaluation of the different epidemiologic interventions employed by the different regions in Sweden and how COVID-19 cases responded to such interventions.

Whereas this study achieved its set objective of identifying the spatiotemporal COVID-19 clusters within the different seasons, the authors understand that the patterns

observed are also influenced by other socio-economic factors as adequately discussed by Drefahl, Wallace [18] and Modig, Ahlbom [35] who noted that being male, having a less individual income, lower education and not being married, all independently predispose one to a higher risk of dying from COVID-19. This position is shared by [Hansson, Albin [36]] who observed variations in COVID-19 cases along immigrant and ethnic lines. As such, the aggregated nature of the data, especially spatially, was a limitation. Certainly, analyzing using individual-level or age-adjusted COVID-19 data would improve the results obtained in this study. This particular aspect is being considered for our subsequent study.

Author Contributions: Conceptualization, Augustus Aturinde and Ali Mansourian; methodology, Augustus Aturinde, Ali Mansourian; software, Augustus Aturinde; validation, Augustus Aturinde; formal analysis, Augustus Aturinde; investigation, Augustus Aturinde, Ali Mansourian; resources, Ali Mansourian; data curation, Augustus Aturinde; writing—original draft preparation, Augustus Aturinde; writing—review and editing, Ali Mansourian; visualization, Augustus Aturinde, Ali Mansourian; supervision, Ali Mansourian; project administration, Ali Mansourian; funding acquisition, Ali Mansourian. All authors have read and agreed to the published version of the manuscript.

Funding: This research received no external funding.

Data Availability Statement: The data leading up to the analysis can be obtained from the Swedish Public Health Agency (Folkhälsomyndigheten), through the web link: https://www.folkhalsomyndigheten.se/smittskydd-beredskap/utbrott/aktuella-utbrott/covid-19/statistik-och-analyser/bekraftade-fall-i-sverige/ (accessed on 30 March 2021).

Acknowledgments: We would wish to extend our gratitude to the Swedish Public Health Agency for providing the data.

Conflicts of Interest: The authors declare no conflict of interest.

References

1. Li, Q.; Guan, X.; Wu, P.; Wang, X.; Zhou, L.; Tong, Y.; Ren, R.; Leung, K.S.; Lau, E.H.; Wong, J.Y. Early transmission dynamics in Wuhan, China, of novel coronavirus–infected pneumonia. *N. Engl. J. Med.* **2020**, *382*, 1199–1207.
2. Spinelli, A.; Pellino, G. COVID-19 pandemic: Perspectives on an unfolding crisis. *J. Br. Surg.* **2020**, *107*, 785–787.
3. Fauci, A.S.; Lane, H.C.; Redfield, R.R. COVID-19—Navigating the uncharted. *Mass Med. Soc.* **2020**, *382*, 1268–1269.
4. Verity, R.; Okell, L.C.; Dorigatti, I.; Winskill, P.; Whittaker, C.; Imai, N.; Cuomo-Dannenburg, G.; Thompson, H.; Walker, P.G.; Fu, H. Estimates of the severity of coronavirus disease 2019: A model-based analysis. *Lancet Infect. Dis.* **2020**, *20*, 669–677.
5. Worldometer. COVID-19 Corona Virus Pandemic. Availabe online: https://www.worldometers.info/coronavirus/ (accessed on 22 April 2022).
6. WHO. WHO Coronavirus (COVID-19) Dashboard. Availabe online: https://covid19.who.int/ (accessed on 30 March 2021).
7. Njenga, M.K.; Dawa, J.; Nanyingi, M.; Gachohi, J.; Ngere, I.; Letko, M.; Otieno, C.; Gunn, B.M.; Osoro, E. Why is there low morbidity and mortality of COVID-19 in Africa? *Am. J. Trop. Med. Hyg.* **2020**, *103*, 564–569.
8. Lalaoui, R.; Bakour, S.; Raoult, D.; Verger, P.; Sokhna, C.; Devaux, C.; Pradines, B.; Rolain, J.-M. What could explain the late emergence of COVID-19 in Africa? *New Microbes New Infect.* **2020**, *38*, 100760.
9. Mariam, S.H. The Severe Acute Respiratory Syndrome Coronavirus-2 (SARS-CoV-2) Pandemic: Are Africa's Prevalence and Mortality Rates Relatively Low? *Adv. Virol.* **2022**, *2022*, 3387784.
10. Shephard, R.J. Immune changes induced by exercise in an adverse environment. *Can. J. Physiol. Pharmacol.* **1998**, *76*, 539–546.
11. Adedokun, K.A.; Olarinmoye, A.O.; Mustapha, J.O.; Kamorudeen, R.T. A close look at the biology of SARS-CoV-2, and the potential influence of weather conditions and seasons on COVID-19 case spread. *Infect. Dis. Poverty* **2020**, *9*, 77.
12. Choi, Y.W.; Tuel, A.; Eltahir, E.A. On the environmental determinants of COVID-19 seasonality. *Geohealth* **2021**, *5*, e2021GH000413.
13. Zoran, M.A.; Savastru, R.S.; Savastru, D.M.; Tautan, M.N.; Baschir, L.A.; Tenciu, D.V. Exploring the linkage between seasonality of environmental factors and COVID-19 waves in Madrid, Spain. *Process Saf. Environ. Prot.* **2021**, *152*, 583–600.
14. Byun, W.S.; Heo, S.W.; Jo, G.; Kim, J.W.; Kim, S.; Lee, S.; Park, H.E.; Baek, J.-H. Is coronavirus disease (COVID-19) seasonal? A critical analysis of empirical and epidemiological studies at global and local scales. *Environ. Res.* **2021**, *196*, 110972.
15. Socialstyrelsen. Statistics on COVID-19. Availabe online: https://www.socialstyrelsen.se/en/statistics-and-data/statistics/statistics-on-covid-19/ (accessed on 30 March 2021).
16. Emborg, H.-D.; Carnahan, A.; Bragstad, K.; Trebbien, R.; Brytting, M.; Hungnes, O.; Byström, E.; Vestergaard, L.S. Abrupt termination of the 2019/20 influenza season following preventive measures against COVID-19 in Denmark, Norway and Sweden. *Eurosurveillance* **2021**, *26*, 2001160.

17. Panneer, S.; Kantamaneni, K.; Akkayasamy, V.S.; Susairaj, A.X.; Panda, P.K.; Acharya, S.S.; Rice, L.; Liyanage, C.; Pushparaj, R.R.B. The Great Lockdown in the Wake of COVID-19 and Its Implications: Lessons for Low and Middle-Income Countries. *Int. J. Environ. Res. Public Health* **2022**, *19*, 610.
18. Drefahl, S.; Wallace, M.; Mussino, E.; Aradhya, S.; Kolk, M.; Brandén, M.; Malmberg, B.; Andersson, G. A population-based cohort study of socio-demographic risk factors for COVID-19 deaths in Sweden. *Nat. Commun.* **2020**, *11*, 5097.
19. Gémes, K.; Talbäck, M.; Modig, K.; Ahlbom, A.; Berglund, A.; Feychting, M.; Matthews, A.A. Burden and prevalence of prognostic factors for severe COVID-19 in Sweden. *Eur. J. Epidemiol.* **2020**, *35*, 401–409.
20. Openshaw, S.; Charlton, M.; Craft, A.W.; Birch, J. Investigation of leukaemia clusters by use of a geographical analysis machine. *Lancet* **1988**, *331*, 272–273.
21. Pullan, R.L.; Sturrock, H.J.; Magalhaes, R.J.S.; Clements, A.C.; Brooker, S.J. Spatial parasite ecology and epidemiology: A review of methods and applications. *Parasitology* **2012**, *139*, 1870–1887.
22. Kulldorff, M.; Heffernan, R.; Hartman, J.; Assunçao, R.; Mostashari, F. A space–time permutation scan statistic for disease outbreak detection. *PLoS Med.* **2005**, *2*, e59.
23. Jones, R.C.; Liberatore, M.; Fernandez, J.R.; Gerber, S.I. Use of a prospective space-time scan statistic to prioritize shigellosis case investigations in an urban jurisdiction. *Public Health Rep.* **2006**, *121*, 133–139.
24. Glatman-Freedman, A.; Kaufman, Z.; Kopel, E.; Bassal, R.; Taran, D.; Valinsky, L.; Agmon, V.; Shpriz, M.; Cohen, D.; Anis, E. Near real-time space-time cluster analysis for detection of enteric disease outbreaks in a community setting. *J. Infect.* **2016**, *73*, 99–106.
25. Kulldorff, M. Prospective time periodic geographical disease surveillance using a scan statistic. *J. R. Stat. Soc. Ser. A (Stat. Soc.)* **2001**, *164*, 61–72.
26. Yin, F.; Li, X.; Ma, J.; Feng, Z. The early warning system based on the prospective space-time permutation statistic. *Wei Sheng Yan Jiu J. Hyg. Res.* **2007**, *36*, 455–458.
27. Tang, X.; Geater, A.; McNeil, E.; Deng, Q.; Dong, A.; Zhong, G. Spatial, temporal and spatio-temporal clusters of measles incidence at the county level in Guangxi, China during 2004–2014: Flexibly shaped scan statistics. *BMC Infect. Dis.* **2017**, *17*, 243.
28. Hohl, A.; Delmelle, E.M.; Desjardins, M.R.; Lan, Y. Daily surveillance of COVID-19 using the prospective space-time scan statistic in the United States. *Spat. Spatio-Temporal Epidemiol.* **2020**, *34*, 100354.
29. Desjardins, M.; Hohl, A.; Delmelle, E. Rapid surveillance of COVID-19 in the United States using a prospective space-time scan statistic: Detecting and evaluating emerging clusters. *Appl. Geogr.* **2020**, *118*, 102202.
30. Gomes, D.; Andrade, L.; Ribeiro, C.; Peixoto, M.; Lima, S.; Duque, A.; Cirilo, T.; Góes, M.; Lima, A.; Santos, M. Risk clusters of COVID-19 transmission in northeastern Brazil: Prospective space–time modelling. *Epidemiol. Infect.* **2020**, *148*, E188.
31. Masrur, A.; Yu, M.; Luo, W.; Dewan, A. Space-time patterns, change, and propagation of COVID-19 risk relative to the intervention scenarios in Bangladesh. *Int. J. Environ. Res. Public Health* **2020**, *17*, 5911.
32. Folkhälsomyndigheten. Confirmed Cases of COVID-19 in Sweden. Availabe online: https://www.folkhalsomyndigheten.se/smittskydd-beredskap/utbrott/aktuella-utbrott/covid-19/statistik-och-analyser/bekraftade-fall-i-sverige/ (accessed on 30 March 2021).
33. Statistics Sweden. Open data for DeSO—Demographic Statistical Areas. Availabe online: https://www.scb.se/en/services/open-data-api/open-geodata/deso--demographic-statistical-areas/ (accessed on 30 March 2021).
34. Sulyok, M.; Walker, M.D. Mobility and COVID-19 mortality across Scandinavia: A modeling study. *Travel Med. Infect. Dis.* **2021**, *41*, 102039.
35. Modig, K.; Ahlbom, A.; Ebeling, M. Excess mortality from COVID-19: Weekly excess death rates by age and sex for Sweden and its most affected region. *Eur. J. Public Health* **2021**, *31*, 17–22.
36. Hansson, E.; Albin, M.; Rasmussen, M.; Jakobsson, K. Stora skillnader i överdödlighet våren 2020 utifrån födelseland (English: Large differences in excess mortality in the spring of 2020 based on country of birth). *Läkartidningen* **2020**, *2920*, 20113.
37. Le, T.H.; Tran, T.P.T. Alert for COVID-19 second wave: A lesson from Vietnam. *J. Glob. Health* **2021**, *11*, 03012.
38. Dellicour, S.; Linard, C.; Van Goethem, N.; Da Re, D.; Artois, J.; Bihin, J.; Schaus, P.; Massonnet, F.; Van Oyen, H.; Vanwambeke, S.O. Investigating the drivers of the spatio-temporal heterogeneity in COVID-19 hospital incidence—Belgium as a study case. *Int. J. Health Geogr.* **2021**, *20*, 29.
39. Venter, Z.S.; Barton, D.N.; Gundersen, V.; Figari, H.; Nowell, M.S. Back to nature: Norwegians sustain increased recreational use of urban green space months after the COVID-19 outbreak. *Landsc. Urban Plan.* **2021**, *214*, 104175.
40. Huang, Z. Spatiotemporal Evolution Patterns of the COVID-19 Pandemic Using Space-Time Aggregation and Spatial Statistics: A Global Perspective. *ISPRS Int. J. Geo-Inf.* **2021**, *10*, 519.